J u r n a l I n d u s t r i S a m u d r a
A Scientific Journal of Industrial Engineering
Journal homepage: https://ejurnalunsam.id/index.php/jis

Effect of Pyrolysis Temperature on Changes in Mass, Dimensions, and Morphology of Cellulose Nanocrystal-Based Carbon

Mahyuni Harahap[1]*, Sahat Fernando Bakara[2], Muhammad Balyan[3], Mutia Amalia[3]
[1] Manufacturing Engineering Technology Study Program, Department of Mechanical Engineering, Medan State Polytechnic, Medan 20155, Indonesia.
[2] Department of Chemistry, Faculty of Science, Technology, and Information, Universitas Sari Mutiara Indonesia, Medan, Indonesia
[3] Welding and Fabrication Engineering Technology Study Program, Department of Mechanical Engineering, Medan State Polytechnic, Medan 20155, Indonesia.
*Corresponding Author: mahyuniharahap1@polmed.ac.id

A R T I C L E I N F O

Pages:
169 – 177

Received:
22 September 2026

Accepted:
10 October 2026

Published:
10 October 2026

ABSTRACT

Cellulose nanocrystals (CNCs) offer renewable alternatives to conventional carbon precursors. This study examined how pyrolysis temperature affects the mass, dimensions (diameter and thickness), and surface morphology of CNC-derived carbon. CNCs with 80% crystallinity were compressed into 13 mm films under 10 tons of pressure and pyrolyzed at 300, 600, and 900 °C under nitrogen at 10 °C/min. Mass and dimensional changes were measured, and morphology was examined using scanning electron microscopy (SEM). Mass loss increased from 49.1% at 300 °C to 73.7% at 600 °C and 76.0% at 900 °C. Diameter and thickness also decreased, with the largest changes occurring between 300 and 600 °C and smaller changes thereafter, suggesting that most thermal decomposition occurred before 600 °C. Carbon appeared chunk-like at 300 °C, porous at 600 °C, and denser, ordered, and flake-like at 900 °C. These findings provide an overview of CNC behavior and morphology as biomass-based carbon precursors.

Keywords: Cellulose Nanocrystals, Pyrolysis, Morphology, SEM, Carbon

1. Introduction

Carbon materials have long attracted attention in materials engineering because of their excellent mechanical properties, low density, and high thermal stability, making them widely used in high-value applications such as aerospace, automotive components, and sporting equipment. Most commercial carbon materials are currently produced from polyacrylonitrile (PAN) and petroleum-based pitch precursors. Although these precursors yield carbon with excellent mechanical properties, they have significant drawbacks: they are derived from non-renewable resources, have high production costs, and, in the case of PAN carbonization, release toxic gases such as hydrogen cyanide [1] [2]. These limitations have driven more intensive research into alternative carbon precursors that are renewable, environmentally friendly, and biodegradable.

Cellulose is the most abundant natural biopolymer on Earth and has long been considered a biomass-based carbon precursor because it is renewable, inexpensive, and has a relatively high carbon content [3],[4]. Among the various forms of cellulose, cellulose nanocrystals (CNCs) have attracted particular attention because they exhibit a much higher degree of crystallinity than conventional

cellulose fibers, owing to the removal of amorphous regions during acid hydrolysis. The highly ordered crystalline structure of CNCs is believed to influence the pathways of carbon-structure formation during pyrolysis, including the tendency to form more ordered graphitic structures than carbon derived from amorphous cellulose [5]. In addition, CNCs are being developed as additives or blended precursors in the production of PAN-based carbon fibers to improve the sustainability of the manufacturing process [6].

Recent studies indicate that CNCs have considerable potential as functional materials and sustainable carbon precursors because they are environmentally friendly, have a high surface area, and can be modified chemically or physically [7]. Previous studies have extensively examined the thermal decomposition of cellulose and the characteristics of carbon produced at various temperatures, particularly carbon yield, chemical structure, and the development of porosity [5],[8],[10]. However, studies specifically linking increasing pyrolysis temperatures to changes in the macroscopic dimensions of CNC films, such as diameter and thickness, and to the stepwise evolution of surface morphology remain limited. Understanding physical changes in mass, dimensions, and surface morphology at different temperatures is essential for explaining the overall conversion of CNCs into carbon materials. Cellulose pyrolysis generally proceeds through several stages, including dehydration at low temperatures, cleavage of glycosidic bonds and formation of volatile compounds at intermediate temperatures, followed by aromatization and formation of more ordered carbon structures at high temperatures [8]. Each stage directly affects the final physical characteristics of the resulting carbon material, including its porosity and surface morphology.

Recent studies have also reported that pyrolysis temperature is one of the most influential factors affecting the development of morphology and pore structure in biomass-based carbon. Increasing the pyrolysis temperature generally increases carbon porosity and surface area up to a certain point, after which the pore structure may shrink because of consolidation and reorganization of the carbon framework at higher temperatures [9],[10]. A similar trend may occur in CNC-based carbon because water and hydroxyl groups in its structure are progressively released during heating. Therefore, this study investigates the effects of pyrolysis temperatures (300 °C, 600 °C, and 900 °C) on changes in the mass, diameter, and thickness of CNC films, as well as the evolution of the surface morphology of the resulting carbon, using scanning electron microscopy (SEM). The findings are expected to provide an initial understanding of the physical behavior of CNCs during thermal conversion into carbon and to support further development of CNCs as sustainable carbon precursors.

2. Methods

The main material used in this study was cellulose nanocrystals (CNCs) with a crystallinity degree of 80% and a diameter of 1–100 nm, obtained from Celluforce, Canada. Nitrogen gas was used to provide an inert atmosphere during pyrolysis. The equipment included a compression press with a 13 mm diameter die, a tube furnace for pyrolysis, an analytical balance, calipers, and a JEOL 6060 SEM. The overall research procedure is presented in the flowchart in Figure 1. CNC films were prepared by weighing 150 mg of CNC powder, placing it in a 13 mm diameter compression die, and applying a pressure of 10 tons to form a flat circular disk.

The CNC films were then pyrolyzed in a tube furnace under a nitrogen atmosphere in the following stages: pre-carbonization from 25 °C to 300 °C at a heating rate of 10 °C/min, followed by an isothermal hold for 1 hour; carbonization from 300 °C to 600 °C at the same heating rate, followed by a 1-hour isothermal hold; and final heating from 600 °C to 900 °C at 10 °C/min, followed by a 1-hour isothermal hold. The heating profile is summarized in Table 1. The percentages of mass loss and dimensional shrinkage were calculated relative to the initial film values before pyrolysis.

Physical changes in CNCs caused by pyrolysis were assessed by measuring film mass, diameter, and thickness before and after heat treatment at each temperature (300 °C, 600 °C, and 900 °C). Three replicates (separate films) were prepared for each temperature, and all data are presented as mean ± standard deviation (SD). Mass was measured using an analytical balance with a precision of 0.01 mg,

while diameter and thickness were measured with calipers (precision: 0.05 mm) at four points on each film. Differences among temperatures were statistically tested using one-way ANOVA followed by Tukey's post hoc test at a significance level of 5% ($p < 0.05$). The surface morphology of the pyrolyzed carbon was analyzed using a JEOL 6060 SEM at an accelerating voltage of 20 kV and magnifications of 500× and 1,000×. Before observation, samples were mounted on adhesive carbon tape and coated with a thin layer of gold using an Emscope SC 500 coater to reduce charging effects during analysis.

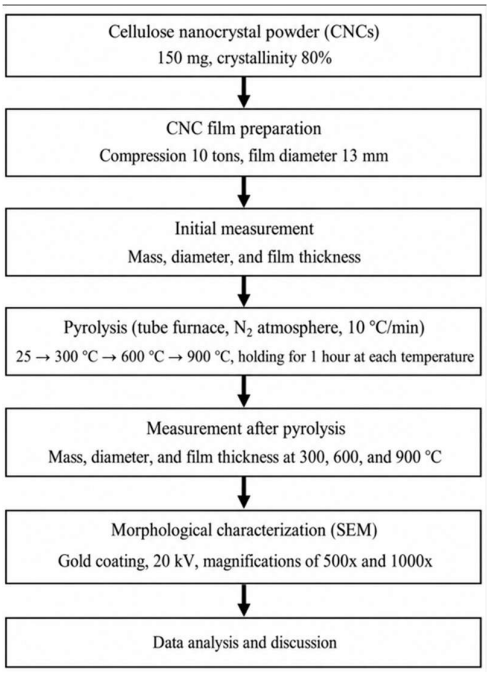


Figure 1. Flowchart of the study on the effect of pyrolysis temperature on changes in the mass, dimensions, and morphology of cellulose nanocrystal-based carbon.

Table 1. Pyrolysis heating profile of cellulose nanocrystal (CNC) films.

Stage	Temperature range (°C)	Heating rate (°C/min)	Isothermal hold	Atmosphere
Pre-carbonization	25–300	10	1 jam	Nitrogen
Carbonization	300–600	10	1 jam	Nitrogen
Final heating	600–900	10	1 jam	Nitrogen

At each final temperature (300, 600, and 900 °C), the results were analyzed using three separate film replicates.

3 Results and Discussion

3.1 Changes in the Mass, Diameter, and Thickness of Cellulose Nanocrystals during Pyrolysis

The pyrolysis of CNCs into carbon involves a series of thermal decomposition reactions that occur progressively as the temperature increases. In general, these stages include the release of free water and dehydration at low temperatures (approximately 100–200 °C); cleavage of glycosidic bonds, producing oligosaccharides and monosaccharides, at intermediate temperatures (200–300 °C); further degradation accompanied by the formation of tar and gases such as CO and CO_2 at 300–500 °C; formation of amorphous and nanocrystalline carbon structures at 500–700 °C; and formation of more ordered carbon structures resembling graphitic layers above 700 °C [5,8]. These stages are quantitatively reflected in the changes in mass and dimensions of the CNC films observed in this study, as shown in Figure 2.

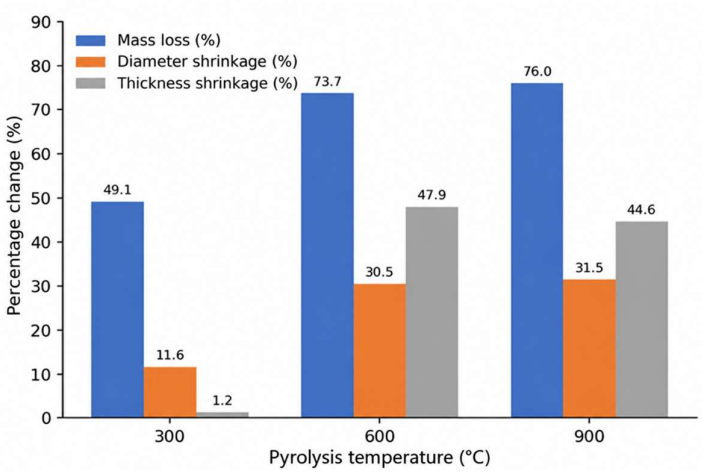


Figure 2. Percentages of mass loss, diameter shrinkage, and thickness shrinkage of cellulose nanocrystal films after pyrolysis at 300 °C, 600 °C, and 900 °C.

As shown in Figure 2, CNC mass loss increased consistently with pyrolysis temperature, amounting to 49.1% at 300 °C, rising to 73.7% at 600 °C, and reaching 76.0% at 900 °C. A similar pattern was observed in diameter shrinkage, which was 11.6% at 300 °C, 30.5% at 600 °C, and 31.5% at 900 °C. Film thickness shrinkage was 1.2% at 300 °C, 47.9% at 600 °C, and 44.6% at 900 °C. These values represent the means of three replicates, with standard deviations shown by the error bars in Figure 2; the differences among temperatures were statistically significant ($p < 0.05$). This pattern indicates that the most substantial changes occurred between 300 and 600 °C, whereas changes from 600 to 900 °C were relatively small; thickness shrinkage even decreased slightly, from 47.9% to 44.6%. A summary of these values, the remaining mass, and the morphological characteristics discussed in Section 3.2 is presented in Table 2.

Table 2. Summary of physical changes and morphology of carbon produced by CNC pyrolysis.

Temperature (°C)	Mass loss (%)	Remaining mass (%)	Diameter shrinkage (%)	Thickness shrinkage (%)	Morphology (SEM)
300	49,1	50,9	11,6	1,2	Chunk-like; rounded to elongated aggregates, relatively smooth surface
600	73,7	26,3	30,5	47,9	Porous; more continuous surface with micro-gaps
900	76,0	24,0	31,5	44,6	Dense; thin flakes (flake-like), reduced porosity

Mass-loss and shrinkage values are the means of three replicates (standard deviations are shown in Figure 2). Remaining mass was calculated as 100% minus mass loss.

This phenomenon is consistent with the thermal decomposition mechanism of cellulose, in which most of the volatile compounds, tar, and gases generated by glycosidic-bond cleavage are released intensively before the temperature reaches 600 °C [11]. Above 600 °C, most of the remaining material is relatively stable carbon residue; therefore, subsequent processes are dominated by structural reorganization (aromatization and formation of a more ordered carbon framework) rather than substantial mass loss [12]. This explains why changes in mass and dimensions between 600 and 900 °C are much smaller than those between 300 and 600 °C. These findings provide an initial indication that 600 °C is a critical point in the thermal conversion of CNCs into carbon, at which most physical

transformations have occurred before the material enters the structural densification stage at higher temperatures.

Although mass loss (from 73.7% to 76.0%) and diameter shrinkage (from 30.5% to 31.5%) increased slightly, thickness shrinkage decreased from 47.9% at 600 °C to 44.6% at 900 °C. This difference of 3.3 percentage points may be explained by several possible factors. First, the difference is relatively small and should be evaluated against replicate variability and the precision of caliper measurements (the error bars in Figure 2); if the difference falls within the standard-deviation range, thickness at 600 °C and 900 °C may be considered statistically equivalent. Second, the CNC films were compressed at 10 tons, potentially storing elastic stress. The release of volatile compounds at 300–600 °C creates pores and microcracks (Figures 3c and 3d), and at higher temperatures, relaxation of residual stress together with the release of remaining gases may cause slight expansion in the thickness direction or prevent further shrinkage. Third, flakes protruding from the surface form at 900 °C (Figures 3e and 3f), increasing surface roughness and potentially making caliper-measured thickness greater than the actual bulk thickness. Because these mechanisms primarily affect the thickness direction, diameter shrinkage (radial direction) continues to increase slightly. Further verification using cross-sectional SEM observations or density measurements is required to identify the dominant mechanism.

3.2 Morphological Analysis of Pyrolysis-Derived Carbon

The surface morphology of carbon produced by CNC pyrolysis at 300 °C, 600 °C, and 900 °C, observed using SEM at magnifications of 500× and 1,000×, is shown in Figure 3. The pyrolysis temperature is indicated in each image panel.

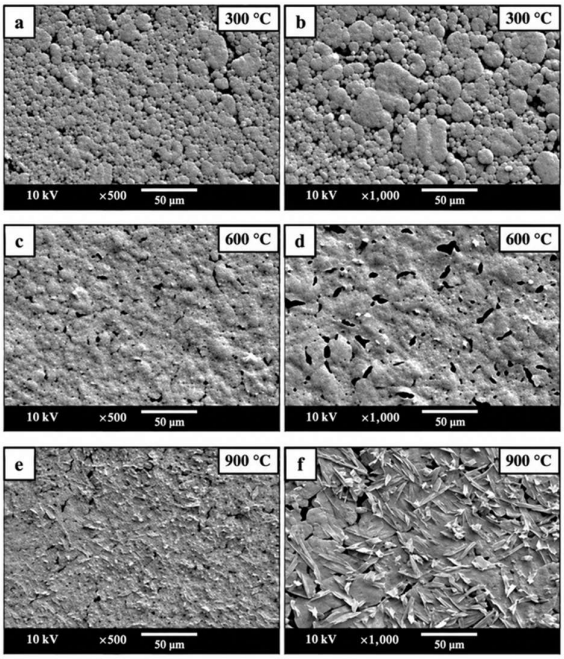


Figure 3. Surface morphology of carbon produced by cellulose nanocrystal pyrolysis at magnifications of 500× and 1,000×: (a,b) 300 °C; (c,d) 600 °C; and (e,f) 900 °C.

At a pyrolysis temperature of 300 °C (Figures 3a and 3b), the carbon surface still exhibits a chunk-like morphology resembling the original CNC structure before heat treatment. This indicates that the material has undergone only the initial stages of thermal decomposition, including dehydration and surface degradation, without significant changes to the carbon framework; consequently, much of the original CNC morphology is retained. At 1,000× magnification (Figure 3b), the surface consists of closely packed rounded to elongated aggregates with clearly defined boundaries and a relatively smooth surface, while fine pores and microcracks are not yet prominent.

At 600 °C (Figures 3c and 3d), the surface morphology changes substantially, characterized by the development of a porous structure with a more uniform pore distribution and an apparently larger surface area than the sample pyrolyzed at 300 °C. This porous structure is consistent with the intensive release of volatile compounds, tar, and gases within this temperature range, leaving voids in the carbon framework after non-carbon components are removed [13]. Increased porosity resulting from volatile release at intermediate pyrolysis temperatures has also been reported for other biomass-derived carbons, such as sawdust-based carbon, which exhibits optimal porosity at around 600 °C before declining at higher temperatures [9]. Morphologically, the separate aggregates observed at 300 °C become a more continuous surface with less distinct aggregate boundaries, accompanied by dark elongated or linear gaps (pores and microcracks) distributed across the surface (Figures 3c and 3d). These changes suggest that, in addition to forming voids through volatile release, the carbon framework may undergo contraction and particle coalescence between 300 and 600 °C.

At 900 °C (Figures 3e and 3f), the carbon morphology develops into a denser, more orderly structure resembling sheets or flakes, with apparently lower porosity than the sample pyrolyzed at 600 °C. This change suggests that at high temperatures the carbon framework undergoes further structural reorganization toward a more ordered arrangement, consistent with aromatization and the formation of graphitic-like structures [14]. The decrease in porosity at high temperatures may result from the collapse of some pore walls and consolidation of the carbon framework. This may reduce surface area while potentially increasing the density and structural order of the material [15]. Morphologically, the surface at 900 °C is dominated by thin flakes protruding in random orientations (Figures 3e and 3f), while the prominent dark gaps observed at 600 °C are substantially reduced. These protruding flakes increase surface roughness and may partly explain why the measured thickness is slightly greater than that at 600 °C.

The correlation between morphology and mass and dimensional data can be summarized as follows. At 300 °C, mass had decreased by 49.1%, while diameter shrank by only 11.6% and thickness by 1.2%. This disparity is consistent with the relatively intact chunk-like morphology (Figures 3a and 3b), suggesting that water and the initial volatile fraction had been released without collapsing the arrangement of CNC particles, so the film dimensions remained relatively stable. At 600 °C, diameter shrinkage (30.5%) and thickness shrinkage (47.9%) increased sharply, alongside a mass loss of 73.7%. At this stage, the release of tar and gases resulting from glycosidic-bond cleavage leaves pores and microcracks (Figures 3c and 3d), while the carbon framework contracts and aggregates move closer together, making the film substantially thinner. The greater thickness shrinkage than diameter shrinkage may be related to the layered structure formed by uniaxial compression, which allows contraction to occur more readily perpendicular to the film plane. At 900 °C, mass loss increased by only 2.3 percentage points and diameter shrinkage by 1.0 percentage point compared with 600 °C, while the morphology changed to flakes (Figures 3e and 3f). This indicates that this stage is dominated by rearrangement of the carbon framework (aromatization and formation of more ordered domains), rather than substantial mass release.

Overall, these morphological observations are consistent with the mass and dimensional changes shown in Figure 2. The substantial changes between 300 and 600 °C are associated with pore formation caused by volatile release, whereas the smaller changes between 600 and 900 °C are associated with structural reorganization toward a denser and more ordered form. These findings reinforce the understanding that pyrolysis temperature is a key parameter determining the final physical characteristics and morphology of CNC-based carbon. They may help guide the selection of processing conditions for specific applications, such as materials requiring high porosity and surface area (600 °C) or materials with a denser and more ordered structure (900 °C).

3.3 Comparison with Previous Studies

The concentration of mass release at intermediate temperatures is consistent with studies of

cellulose pyrolysis kinetics and mechanisms. Lin et al. [16] reported that the initial stage of cellulose pyrolysis involves depolymerization of solid cellulose into levoglucosan, while char forms through polymerization of pyrolysis products; they also found that the intrinsic kinetics of cellulose pyrolysis are independent of the heating rate. These findings help explain why most of the mass loss in this study (73.7% at 600 °C) had occurred before the temperature reached 900 °C, while the material remaining between 600 and 900 °C was primarily char undergoing structural rearrangement. Because the heating rate and isothermal holding time were kept constant (Table 1), differences among samples can be attributed mainly to the final pyrolysis temperature.

In addition to temperature, the surface chemistry of CNCs may also affect the results. Commercial CNCs are commonly produced by sulfuric acid hydrolysis, which leaves sulfate ester groups on the nanocrystal surface [17]. Roman and Winter [18] reported that sulfate groups introduced by sulfuric acid hydrolysis reduce the thermal stability of bacterial cellulose nanocrystals. In nanoplates made from CNCs, these sulfate groups have also been associated with relatively high char yields compared with microcrystalline cellulose [19], and the thermal degradation behavior of sulfated CNCs has also been investigated by Wang et al.[20]. The sulfate content of the CNCs used in this study was not analyzed; therefore, its possible role in the rapid mass loss between 300 and 600 °C remains speculative and requires verification through thermogravimetric and elemental analyses.

The remaining mass in this study was 26.3% at 600 °C and 24.0% at 900 °C (Table 2). Stoichiometrically, the carbon content of cellulose is only about 44%, so a remaining mass of 24.0% is approximately half of that theoretical limit; this value still exceeds the actual carbon content because the residue at 900 °C contains some hydrogen and oxygen. Low carbon yield is one of the main limitations of cellulose precursors compared with PAN, as reviewed by Dumanlı and Windle [21]. Therefore, strategies to increase yield, including control of low-temperature heat-treatment stages, remain important for the development of CNC-based carbon.

The carbon structure formed at 900 °C should also be distinguished from well-ordered graphite. Lewandowska et al. [22] obtained oriented turbostratic carbon domains from regenerated cellulose fibers graphitized at temperatures up to 2,000 °C. In the present study, heating reached only 900 °C and observations were limited to surface morphology; therefore, the term structural rearrangement toward a more ordered structure does not imply that graphite was formed. Eom et al. [5] also showed that direct carbonization of CNCs in an inert atmosphere produces an irregular morphology due to molecular melting, whereas oxidative stabilization at 250 °C preserves a needle-like structure. The loss of aggregate boundaries at 600 °C and the formation of flakes at 900 °C in this study are consistent with these trends and indicate that low-temperature stabilization is a variable worth testing in future research.

The findings provide an initial basis for selecting pyrolysis temperatures according to application requirements. The porous carbon produced at 600 °C, with its larger apparent surface area, is more suitable as a starting material for adsorbents or activated carbon. This is consistent with Lee et al. [19], who found that carbon derived from CNC nanoplates can be activated to produce microporous carbon with a surface area of up to 1,310.6 m^2/g. In contrast, the denser and more orderly carbon produced at 900 °C may be more relevant for applications requiring greater density and structural order. Because the changes from 600 to 900 °C are relatively small, selecting 600 °C may also reduce process energy consumption if the required properties have already been achieved.

4 Conclusion

In conclusion, pyrolysis temperature significantly affects the mass, dimensions, and morphology of carbon produced from cellulose nanocrystals (CNCs). Mass loss and shrinkage in CNC film diameter and thickness increased with pyrolysis temperature, with the most substantial changes occurring between 300 and 600 °C, while changes from 600 to 900 °C were relatively small. Thickness shrinkage decreased slightly from 47.9% at 600 °C to 44.6% at 900 °C, possibly because of relaxation of residual

compression stress, gas release, and the formation of flakes on the surface. This indicates that most thermal decomposition and volatile-compound release had occurred before the temperature reached 600 °C. SEM morphological analysis showed characteristic structural evolution with increasing temperature: a chunk-like structure resembling the original CNCs at 300 °C, a porous structure with a larger apparent surface area at 600 °C, and a denser, more ordered, sheet-like structure at 900 °C due to reorganization of the carbon framework toward a more ordered arrangement. This study provides a useful initial understanding for developing CNCs as sustainable biomass-based carbon precursors. Further characterization of crystal structure, porosity, and thermal properties, along with studies of low-temperature stabilization, is required to confirm their application potential.

Declaration of AI Use

The author states that ChatGPT was used to a limited extent to assist with language editing and grammar checking during the preparation of the manuscript. The author bears full responsibility for all scientific content, data analysis, interpretation of results, and conclusions. All editing assisted by ChatGPT has been reviewed and verified by the author.

Author Contributions

Conceptualization, Mahyuni Harahap, and Sahat Fernando Bakara; methodology, Mahyuni Harahap and Muhammad Balyan; formal analysis, Mahyuni Harahap, and Atikah Amatullah; investigation, Mahyuni Harahap; data curation, Difana Meilani; writing—original draft preparation, Mahyuni Harahap; writing— review and editing, Sahat Fernando Bakara and Mutia Amalia. All authors have read and agreed to the published version of the manuscript.

Funding Declaration

This research was conducted without specific funding support from government agencies, private institutions, or other organizations. All research costs were borne independently by the author.

Conflict of Interest Declaration: The authors declare no conflict of interest.

References

[1] Y. Xu, Y. Liu, S. Chen, and Y. Ni, "Current overview of carbon fiber: Toward green sustainable raw materials," *BioResources*, vol. 15, no. 3, pp. 7234–7259, Jun. 2020, doi: https://doi.org/10.15376/biores.15.3.Xu.

[2] M. Harahap, N. Daulay, D. Zebua, and S. Gea, "Nanofiber Cellulose/Lignin from Oil Palm Empty Fruit Bunches and the Potential for Carbon Fiber Precursor Prepared by Wet-spinning," *Int. J. Technol.*, vol. 14, no. 1, pp. 152–161, 2023, doi: https:// doi.org/10.14716/ijtech.v14i1.5082.

[3] N. D. Le, R. J. Varley, M. Hummel, M. Trogen, and N. Byrne, "A review of future directions in the development of sustainable carbon fiber from bio-based precursors," *Mater. Today Sustain.*, vol. 20, 2022, doi: https:// doi.org/ 10.1016/j.mtsust.2022.100251.

[4] S. Gea, A. H. Siregar, E. Zaidar, M. Harahap, D. P. Indrawan, and Y. A. Perangin-Angin, "Isolation and characterisation of cellulose nanofibre and lignin from oil palm empty fruit bunches," *Materials (Basel).*, vol. 13, no. 10, 2020, doi: https:// doi.org/ 10.3390/ma13102290.

[5] Y. Eom, S. M. Son, Y. E. Kim, J.-E. Lee, S.-H. Hwang, and H. G. Chae, "Structure evolution mechanism of highly ordered graphite during carbonization of cellulose nanocrystals," *Carbon N. Y.*, vol. 150, pp. 142–152, Sep. 2019, doi: https:// doi.org/ 10.1016/j.carbon.2019.05.007.

[6] I. Kruppke, F. Sherif, M. Richter, and C. Cherif, "Development of Porous-Polyacrylonitrile-Based Fibers Using Nanocellulose Additives as Precursor for Carbon Fiber Manufacturing," *Polymers (Basel).*, vol. 15, no. 3, p. 565, Jan. 2023, doi: https:// doi.org/ 10.3390/polym15030565.

[7] M. N. Norizan *et al.*, "Nanocellulose-Based Nanocomposites for Sustainable Applications: A Review," *Nanomaterials*, vol. 12, no. 19, p. 3483, Oct. 2022, doi: https:// doi.org/

10.3390/nano12193483.

[8] M. M. Sabzehmeidani, S. Mahnaee, M. Ghaedi, H. Heidari, and V. A. L. Roy, "Carbon based materials: a review of adsorbents for inorganic and organic compounds," *Mater. Adv.*, vol. 2, no. 2, pp. 598–627, 2021, doi: https:// doi.org/ 10.1039/D0MA00087F.

[9] M. Arman, Z. Sabara, and T. Arief, "The Effect of Pyrolysis Temperature on Sawdust-Biomass Activated Carbon Using NaOH and NaCl Activators," *Eng. J.*, vol. 28, no. 8, p. 1, Aug. 2024, doi: https:// doi.org/ 10.4186/ej.2024.28.8.1.

[10] P. K. Mubari, T. Beguerie, M. Monthioux, E. Weiss-Hortala, A. Nzihou, and P. Puech, "The X-ray, Raman and TEM Signatures of Cellulose-Derived Carbons Explained," *C*, vol. 8, no. 1, p. 4, Jan. 2022, doi: https:// doi.org/ 10.3390/c8010004.

[11] X. Zhang, Y. Zhang, S. Zhang, L. Yao, and Y. Hao, "Lignocellulosic biomass pyrolysis: A review on the pretreatment and catalysts," *Fuel Process. Technol.*, vol. 279, p. 108352, Dec. 2025, doi: https:// doi.org/ 10.1016/j.fuproc.2025.108352.

[12] J. Kujawska, W. Cel, B. Charmas, and D. Szala, "Effect of Pyrolysis Temperature on Chemical Structure and Thermal Stability of Digestate-Based Biochar," *Energies*, vol. 19, no. 4, p. 1043, Feb. 2026, doi: https:// doi.org/ 10.3390/en19041043.

[13] R. Kumar Mishra, B. Singh, and B. Acharya, "A comprehensive review on activated carbon from pyrolysis of lignocellulosic biomass: An application for energy and the environment," *Carbon Resour. Convers.*, vol. 7, no. 4, p. 100228, Dec. 2024, doi: https:// doi.org/ 10.1016/j.crcon.2024.100228.

[14] Z. Liang *et al.*, "Molecular structure and evolution mechanism of shale kerogen: Insights from thermal simulation and spectroscopic analysis," *J. Anal. Appl. Pyrolysis*, vol. 181, p. 106648, Aug. 2024, doi: https:// doi.org/ 10.1016/j.jaap.2024.106648.

[15] J. Alcañiz-Monge, G. Trautwein, M. Pérez-Cadenas, and M. C. Román-Martínez, "Effects of compression on the textural properties of porous solids," *Microporous Mesoporous Mater.*, vol. 126, no. 3, pp. 291–301, Dec. 2009, doi: https:// doi.org/ 10.1016/j.micromeso.2009.06.020.

[16] S. Hameed, A. S. Wagh, A. Sharma, V. Pareek, Y. Yu, and J. B. Joshi, "Kinetic modelling of pyrolysis of cellulose using CPD model: effect of salt," *J. Therm. Anal. Calorim.*, vol. 147, no. 17, pp. 9763–9777, Sep. 2022, doi: https:// doi.org/ 10.1007/s10973-021-11192-5.

[17] Y. Habibi, L. A. Lucia, and O. J. Rojas, "Cellulose Nanocrystals: Chemistry, Self-Assembly, and Applications," *Chem. Rev.*, vol. 110, no. 6, pp. 3479–3500, Jun. 2010, doi: https:// doi.org/ 10.1021/cr900339w.

[18] A. Merlini, C. Claumann, A. W. Zibetti, A. Coirolo, T. Rieg, and R. A. F. Machado, "Kinetic Study of the Thermal Decomposition of Cellulose Nanocrystals with Different Crystal Structures and Morphologies," *Ind. Eng. Chem. Res.*, vol. 59, no. 30, pp. 13428–13439, Jul. 2020, doi: https:// doi.org/ 10.1021/acs.iecr.0c01444.

[19] S. Lee, M. E. Lee, M. Y. Song, S. Y. Cho, Y. S. Yun, and H.-J. Jin, "Morphologies and surface properties of cellulose-based activated carbon nanoplates," *Carbon Lett.*, vol. 20, pp. 32–38, Oct. 2016, doi: https:// doi.org/ 10.5714/CL.2016.20.032.

[20] K. N. M. Amin, A. Hosseinmardi, D. J. Martin, and P. K. Annamalai, "A mixed acid methodology to produce thermally stable cellulose nanocrystal at high yield using phosphoric acid," *J. Bioresour. Bioprod.*, vol. 7, no. 2, pp. 99–108, May 2022, doi: https:// doi.org/ 10.1016/j.jobab.2021.12.002.

[21] A. G. Dumanlı and A. H. Windle, "Carbon fibres from cellulosic precursors: a review," *J. Mater. Sci.*, vol. 47, no. 10, pp. 4236–4250, May 2012, doi: https:// doi.org/ 10.1007/s10853-011-6081-8.

[22] A. E. Lewandowska, C. Soutis, L. Savage, and S. J. Eichhorn, "Carbon fibres with ordered graphitic-like aggregate structures from a regenerated cellulose fibre precursor," *Compos. Sci. Technol.*, vol. 116, pp. 50–57, Sep. 2015, doi: https:// doi.org/ 10.1016/j.compscitech.2015.05.009.